B3LYP, Hybrid Density Functional Studies of the Durosemiquinone Radical: The Effect of Symmetrical and Asymmetrical Hydrogen Bonding on Spin Densities and Hyperfine Couplings

Patrick J. O'Malley

Department of Chemistry, UMIST, Mancheter M60 1QD, U.K.

Received: July 29, 1997; In Final Form: October 17, 1997[⊗]

Hybrid density functional calculations utilizing the B3LYP functional are used to calculate geometries spin densities, and isotropic and anisotropic hyperfine couplings for the durosemiquinone anion radical. Spin densities and hyperfine couplings are compared for the free ion, a symmetrical hydrogen-bonded complex with four methanol molecules, and an asymmetrical hydrogen-bonded complex with methyl imidazole. A redistribution of unpaired electron spin density from the oxygen and ring carbon atom positions to the carbonyl carbon atom position is shown to occur on symmetrical hydrogen bond formation. In the asymmetrical case a redistribution of spin density within the semiquinone ring system occurs. The asymmetric hydrogen-bonding data are in good accord with experimental values obtained for the durosemiquinone radical substituted into the Q_a site of the photosynthetic bacterium *Rhodobacter sphaeroides*. Excellent agreement is observed between calculated and experimentally determined hyperfine coupling constants.

Introduction

Quinones are ubiquitous to living systems and represent important cofactors for electron transfer in photosynthesis and respiration.[1] In photosynthesis, for example, quinones act as electron acceptors in the initial charge separation. For both bacterial and higher plant photosystem 2, two quinones termed Q_a and Q_b act in concert to enable efficient charge separation to take place.[2] Q_a is initially reduced to form the semiquinone anion radical. This then forwards its electron to Q_b, forming the Q_b semiquinone anion radical. On further charge separation, Q_a accepts another electron to form the semiquinone anion radical again. This electron is then passed on to the already reduced Q_b to form quinol QH_2, which leaves the protein site to be replaced by another quinone molecule from a quinone pool nearby.

Q_a and Q_b are often identical quinones: plastoquinone in higher plants and ubiquinone in bacterial systems. In the photosynthetic bacterium *Rhodobacter sphaeroides* a variety of other quinones including duroquinone have been substituted into the Q_a binding site.[3] A variety of spectroscopic methods, most notably, EPR, ENDOR, FTIR, and NMR, have been used to investigate differences between the Q_a and Q_b quinones.[4−6] Differences in the hydrogen-bonding ability of both quinones is generally put forward for the differing functions observed; i.e., specific hydrogen bonds to nearby amino acid residues are able to tailor the quinone to perform a specific function. EPR and ENDOR studies have afforded a detailed look at the electronic structure of the semiquinone anion radical formed in the Q_a and Q_b sites. Differences in the nature of the hydrogen-bonding interactions of both semiquinones have been put forward to explain the different spectroscopic manifestations observed.

In this study we use modern density functional methods to examine the structure, spin density distribution, and hyperfine couplings of the durosemiquinone anion radical both in its free and hydrogen-bonded states. Our previous studies have demonstrated the excellent data concerning spin densities and hyperfine couplings that can be obtained for the unsubstituted *p*-benzosemiquinone radical using hybrid density functional methods.[7,8] The durosemiquinone anion radical has been studied extensively by EPR and ENDOR method in both liquid and frozen alcohol solution.[9] The semiquinone radical has also been generated in the Q_a binding site of *Rb. sphaeroides* and investigated by EPR and ENDOR.[3,10]

Hybrid density functional methods, particularly the B3LYP functional, are increasingly being shown to provide excellent electronic structures for nonradicals and radicals alike.[11−13] They are uniquely capable of giving highly accurate descriptions of free radical properties such as isotropic and anisotropic hyperfine coupling constants.[13,14] For free radical properties Hartree−Fock based methods perform very poorly.[14] Nuclear hyperfine couplings consist of isotropic (Fermi contact) and anisotropic (dipolar) terms. In the electronic structure calculation both are calculated separately. Experimentally, in liquid solution, rapid tumbling leads to the elimination of the anisotropic components and the isotropic value is obtained in isolation. For solid-state studies, both the isotropic and anisotropic terms contribute to the coupling and the total tensor is the experimental observable.

For calculation purposes the 3×3 hyperfine interaction tensor can be separated into its isotropic (spherically symmetric) and anisotropic (dipolar) components. To first-order isotropic hyperfine interactions, $A_{iso}(N)$ are related to the spin densities, $\rho^s(r_N)$, at the corresponding nuclei by

$$A_{iso}(N) = (8\pi/c)g_e g_N \beta\beta_N \rho^s(r_N)$$

The anisotropic components are derived from the classical expression of interacting dipoles

$$A_{ij}(N) = g_e g_N \beta\beta_N \sum \boldsymbol{P}^{\alpha-\beta}{}_{\mu\nu} \langle \varphi_\mu | r^{-5}{}_{kN} (r^2{}_{kN}\delta_{ij} - 3r_{kNi}r_{kNj}) | \varphi_\nu \rangle$$

[⊗] Abstract published in *Advance ACS Abstracts,* December 1, 1997.

S1089-5639(97)02467-5 CCC: $15.00
Published on Web 01/01/1998

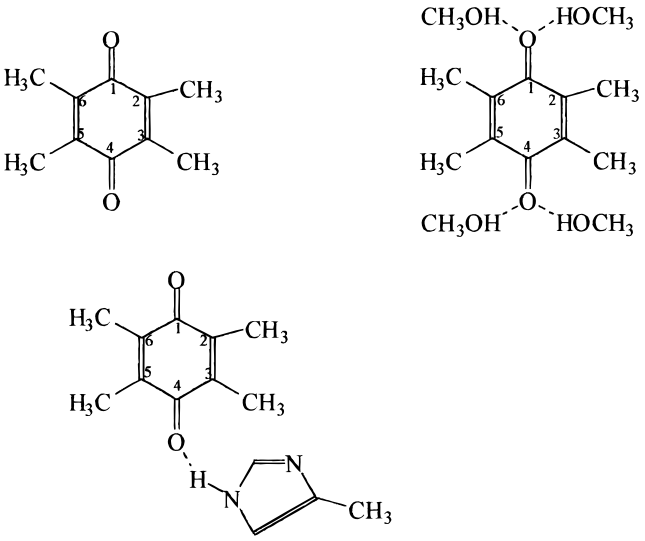

Figure 1. Complexes with atom numbering scheme used: (top left) DQ, (top right) DQ−4CH_3OH, and (bottom) DQ−IM.

TABLE 1: Optimized Bond Distances (angstroms) for the Radical Complexes of Figure 1

bond	DQ	DQ−4CH_3OH	DQ−IM
C1−O1	1.25	1.26	1.25
C4−O4	1.25	1.26	1.27
C1−C2	1.46	1.45	1.46
C2−C3	1.37	1.37	1.37
C3−C4	1.46	1.45	1.45
C4−C5	1.46	1.45	1.45
C5−C6	1.37	1.37	1.37
C6−C1	1.46	1.45	1.46
O1−H(hb)		1.78	
O4−H(hb)		1.78	1.74

The isotropic component can be obtained from the Fermi contact analysis given by most modern electronic structure programs. The anisotropic components can be obtained from the spin only electric field gradient tensors.

Methods

The radicals studied are shown in Figure 1. The free non-hydrogen-bonded radical was studied in addition to the symmetrical hydrogen-bonding situation of two methanol molecules per each carbonyl, DQ−4CH_3OH, and the asymmetrical hydrogen-bonding situation where one of the carbonyl oxygens is hydrogen bonded to a methyl imidazole molecule, DQ−IM.

For the calculation of spin densities and hyperfine couplings, we utilized the B3LYP hybrid functional[15] as implemented in GAUSSIAN94[16] combined with the EPR-II basis set. The appropriateness of the EPR-II basis set for hyperfine coupling calculations has been recently demonstrated by us.[7] The geometries for the complexes were optimized at the semiempirical PM3 level using SPARTAN,[17] which was also used to generate the spin density surfaces. No symmetry constraints were imposed during the calculations. For DQ−4CH_3OH the slight asymmetry observed for the calculated anisotropic and isotropic hyperfine coupling constants is a reflection of this as it permitted slightly inequivalent orientations for the hydrogen-bonding methanol molecules to be allowed.

Results and Discussion

(a) Geometries. Selected optimized bond distances of all three complexes are given in Table 1. Of particular note in the lengthening of the carbonyl bond from 1.24 to 1.27 Å on hydrogen bond formation. It is also of note that in contrast to the *p*-benzosemiquinone case[7,13] the hydrogen bond hydrogen donors are shifted to the quinone plane and interaction occurs above or below the quinone plane as demonstrated in Figure 2. This confirms our conclusions reached previously on the basis of ENDOR studies[9] and is attributable to the bulky methyl group substituents that prevent hydrogen bond formation in the quinone plane.

Figure 2. Side view of the DQ−4CH_3OH radical complex demonstrating the out of plane orientation of the hydrogen bond donor atoms of the methanol molecules.

(b) Spin Density Surfaces. The spin density surfaces at 0.01 e/au^3 are shown in Figure 3. A symmetrical distribution of spin density is observed for the non-hydrogen-bonded and DQ−4CH_3OH radicals. Unpaired spin density is concentrated at the oxygen atoms. Hydrogen bonding leads to a substantial spin density increase at the C1 and C4 oxygen atoms. For the DQ−IM complex an asymmetrical spin density distribution is observed. Hydrogen bonding to the O4 oxygen atom leads to increased spin density at the C4, C2, and C6 positions with a corresponding decrease at C3 and C5. These spin density plots are discussed below along with the anisotropic hyperfine coupling constants.

(c) Anisotropic Hyperfine Couplings. The anisotropic hyperfine coupling tensor principal values are given in Table 2. These are a direct reflection of the spin density plots in Figure 3. The magnitude of the values observed are a reflection of the concentration of spin density around the nucleus concerned, and the symmetry of the tensor components is a reflection of the symmetry of the spin density distribution around the nucleus. Taking the O1 position first, we can see that for all three radicals an essentially axial tensor is observed. From Figure 3 we can see that the spin density surrounding the O1 atom is of cylindrical nature and hence gives rise to the observed axial symmetry with the principal value lying along the out-of-plane axis. The decrease in the absolute magnitude of the values for the DQ−4CH_3OH case reflects a decrease in the spin density at this position caused by the hydrogen bond formed at this oxygen atom. For the O4 oxygen atom hydrogen bonding in DQ−4CH_3OH and DQ−IM leads to a decrease in spin density at O4 and as a result a lowering in the ^{17}O anisotropic hyperfine coupling values. Hydrogen bonding leads to a significant increase in the C1 and C4 anisotropic ^{13}C hyperfine coupling values for the DQ−4CH_3OH case reflecting the increased spin density at the carbonyl carbom atoms on hydrogen bond formation. For the DQ−IM radical the anisotropic coupling of C4 (near the hydrogen bond) is increased in a similar fashion as for DQ−4CH_3OH. For C1 a more complex situation exists. Here, as shown in Figure 3, for both the non-hydrogen-bonded radical and DQ−IM a region of relatively low spin density exists compared with the values on the surrounding atoms. In such a position, as discussed previously for the *p*-benzosemiquinone radical,[7] this neighboring spin density will contribute substantially to the anisotropic couplings and lead to deviations from axial symmetry. The spin density contour, Figure 3, indicates that the spin density around the C1 atom is similar for DQ and

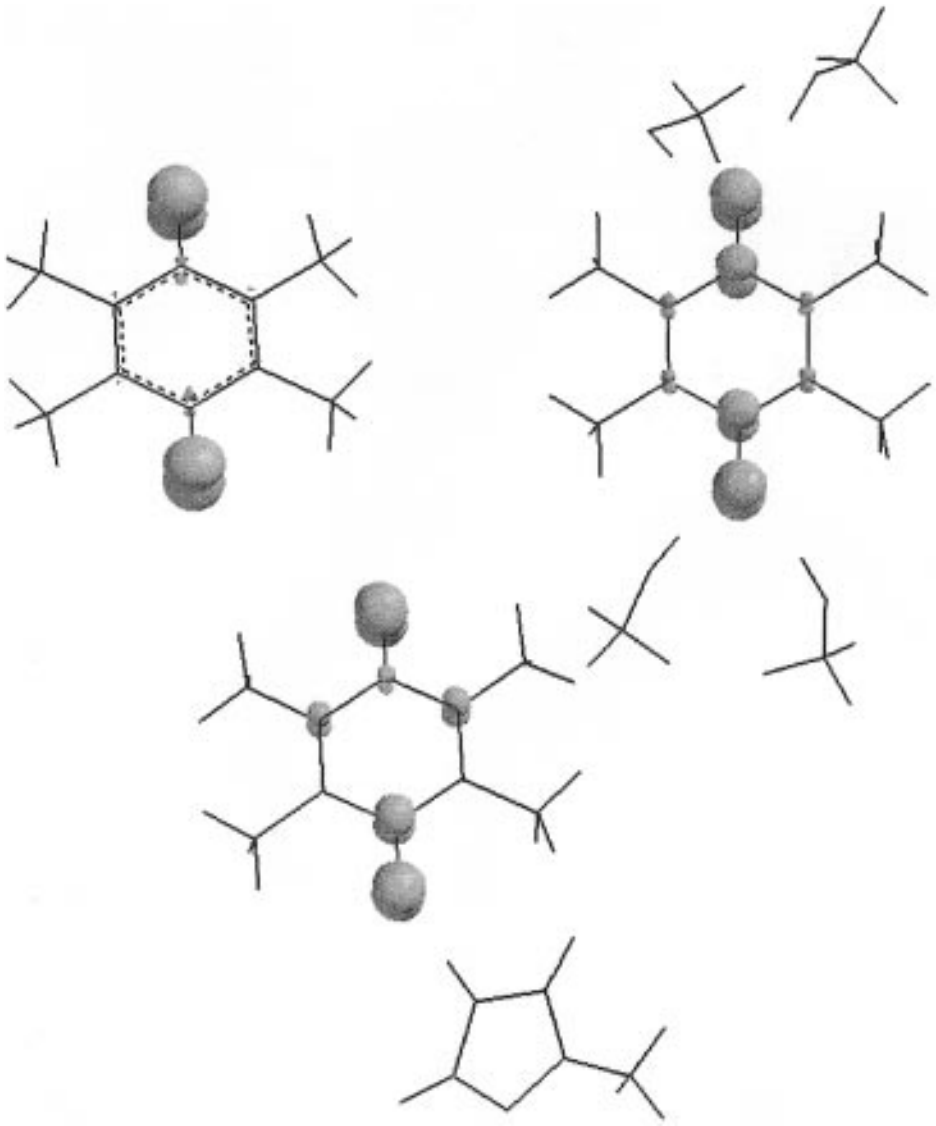

Figure 3. Unpaired spin density surfaces (0.01 e/au^3) for the radicals of Figure 1: (top right) DQ, (top left) DQ−4CH_3OH, and (bottom) DQ−IM. Radical orientation and numbering as given in Figure 1.

DQ−IM. The difference in the anisotropic couplings observed, Table 2, is attributable to the much larger spin density value surrounding C2 and C6 for DQ−IM. For the C2, C3, C5, and C6 position no significant changes are observed in the anisotropic hyperfine couplings in going from the free to the symmetrical hydrogen-bonded situation for DQ−4CH_3OH. For DQ−IM, however, the C2 and C6 positions are increased whereas the C3 and C5 positions are decreased. This is again explained by the spin density plots of Figure 3 where one-sided hydrogen bonding to the imidazole leads to the redistribution of spin density from C3 and C5 to C2 and C6. Hence the C2 and C6 positions have large and axial anisotropic hyperfine tensors because they are determined by the spin density at the nuclei in question. The C3 and C5 principal values deviate substantially from axial behavior. At these positions the spin density is low, and neighboring atom spin density will contribute to the anisotropic coupling removing the cylindrical symmetry of the interaction.

(d) Isotropic Hyperfine Couplings. Isotropic hyperfine couplings arise due to the appearance of spin density directly at the nucleus in question. To first order the unpaired electron in the radicals of this study are located in a π type orbital, and as such no spin density should appear at the nuclei involved. The spin density at the nuclei arises due to spin polarization, which in essence leads to an unpairing in the formally paired s electrons in contact with the nuclei. The interaction between this unpaired spin and the magnetic moment of the nuclei gives rise to the isotropic term. In Table 3 the isotropic couplings calculated for the nuclei in Table 2 are presented. Our main focus will be on the variations brought about by hydrogen bonding for DQ−4CH_3OH and DQ−IM.

We will discuss the O1, O4 and C1, C4 atoms together. Relatively small changes are observed for the oxygen atom isotropic couplings on hydrogen bond formation, whereas large variations are brought about to the C1 and C4, ^{13}C isotropic couplings. Spin polarization by the atom's own π spin leads to excess α (positive) s spin density at the nucleus and contributes positively to the isotropic coupling.[18] Polarization by neighboring π spin will also occur. Spin polarization by the neighboring π spin density will lead to excess β (negative) contributions to the isotropic coupling.[18]

As discussed above on symmetrical hydrogen bond formation, for DQ−4CH_3OH, a substantial increase in spin density at the C1 and C4 positions is observed. This will give rise to a positive

TABLE 2: Principal Values (T_{11}, T_{22}, T_{33}) of the Anisotropic Hyperfine Coupling Tensor for the Radicals of Figure 1. All Values Given in MHz

position	DQ	DQ−4CH_3OH	DQ−IM
O1	−77.6	−64.8	−77.3
	39.1	32.2	38.4
	37.4	32.6	38.8
O4	−77.6	−64.7	−65.5
	39.1	32.3	32.5
	37.4	32.3	33.1
C1	16.3	27.6	13.6
	−10.1	−12.3	−4.9
	−6.3	−15.1	−8.7
C4	16.3	27.2	27.6
	−10.1	−12.3	−12.4
	−6.3	−15.0	−15.1
C2	13.8	12.1	19.8
	−5.8	−5.8	−9.8
	−6.2	−6.3	−10.1
C3	13.8	12.1	7.5
	−5.8	−5.8	−3.5
	−6.2	−6.3	−4.1
C5	13.8	12.1	7.3
	−5.8	−5.8	−3.1
	−6.2	−6.3	−4.1
C6	13.8	11.7	17.5
	−5.8	−5.6	−8.6
	−6.2	−6.1	−8.9
C_{Me}(2)	0.7	0.7	0.8
	−0.3	−0.4	−0.4
	−0.3	−0.4	−0.5
C_{Me}(3)	0.7	0.7	0.8
	−0.3	−0.4	−0.5
	−0.3	−0.4	−0.2
C_{Me}(5)	0.7	0.7	0.8
	−0.3	−0.4	−0.5
	−0.3	−0.4	−0.2

TABLE 3: Isotropic Hyperfine Coupling Values for Radicals of Figure 1, in MHz

position	DQ	DQ−4CH_3OH	DQ−IM
O1	−19.7	−18.1	−18.9
O4	−19.7	−17.9	−18.3
C1	−8.4	−0.6	−12.0
C4	−8.4	−0.7	0.5
C2	−0.9	−2.0	4.8
C3	−0.9	−2.0	−5.8
C5	−0.9	−2.0	−5.3
C6	−0.9	−2.1	3.6
C_{Me}(2)	−4.2	−3.5	−5.6
C_{Me}(3)	−4.2	−3.5	−2.5
C_{Me}(5)	−4.2	−3.5	−2.6
C_{Me}(6)	−4.2	−3.5	−5.1

contribution to the C1 and C4 ^{13}C isotropic coupling, and as a result the increase in isotropic coupling from −8.4 to −0.7 MHz can be attributed to this change. The decrease in unpaired spin at the oxygen positions on hydrogen formation will also contribute by lowering the negative contribution to the carbonyl carbon isotropic hyperfine coupling. For the asymmetrical DQ−IM radical the C1 ^{13}C isotropic coupling is decreased compared with the non-hydrogen-bonded case whereas the C4 position increases substantially from −8.3 to +0.5 MHz. Again these changes are a reflection of the spin density changes shown in Figure 3. For the C4 position the presence of a hydrogen bond causes a substantial increase in π spin density at the C4 position. As outlined above this give rise to a positive contribution to the C4 isotropic coupling. In addition the C3 and C5 spin density is reduced compared with the non-hydrogen-bonded case and as such their negative contribution to the C4 ^{13}C isotropic coupling is reduced even with respect to the symmetrical hydrogen-bonded case. For the C1 position the large negative coupling of −12.0 MHz can be attributed to the decrease in π spin at the C1 atom itself (decreased positive contribution) plus the increase in π spin at the neighboring C2 and C6 atom positions. The substantial π spin at these neighboring positions will contribute in a negative sense to the C1 isotropic coupling, hence providing a rationale for the observed large negative coupling.

TABLE 4: Comparison of Theoretical, DQ−4CH_3OH, and Experimental (Alcohol Solvent) Isotropic Hyperfine Coupling Values[a]

	isotropic coupling			isotropic coupling	
position	exptl	calcd	position	exptl	calcd
C1	2.99	−0.7	C_{Me}	−3.8	−3.5
C2	−2.0	−2.0	H	5.3	5.0

[a] Experimental values taken from refs 19 and 20.

The isotropic couplings for C2, C3, C5, and C6 decrease by about 1 MHz on symmetrical hydrogen bond formation, DQ−4CH_3OH (Table 3). The π spin density at these positions changes little on hydrogen bond formation; hence, this positive contribution to the isotropic couplings should remain similar on hydrogen bond formation. The π spin density at the C1 and C4 positions increases significantly on hydrogen bond formation and will contribute negatively to the C2, C3, C5, and C6 isotropic couplings. The decrease of 1 MHz can therefore be principally attributed to such an effect. For the asymmetrical hydrogen-bonded case, DQ−IM, a large positive ^{13}C isotropic coupling is observed for C2 and C6 whereas a large negative coupling is observed for C3 and C5. This again is in accord with the π spin density distribution of Figure 3. The C2 and C6 positions have a large π spin density, which will give rise to a correspondingly large positive contribution to their respective ^{13}C isotropic couplings. For the C3 and C5 positions a very low π spin density is calculated; see Figure 3. As a result the positive contribution to their isotropic coupling is small. By contrast the neighboring atom positions, C4, C2, and C6, have large π spin densities and as a result will contribute significantly in a negative sense to the C3 qnd C5 isotropic couplings, hence explaining the large negative coupling observed.

(e) Comparison with Experimental Findings. Many experimental electron paramagnetic resonance (EPR) and electron nuclear double resonance (ENDOR) studies of the durosemiquinone anion radical have been performed.[9,19,20] These have been performed in liquid alcohol solutions, in frozen alcohol solutions, and also for reaction center complexes of *Rb. sphaeroides* in which DQ has been substituted into the Q_a binding sites.[3,10] The liquid solution EPR or ENDOR studies can only supply the isotropic hyperfine couplings, as the anisotropic components are averaged out by rapid tumbling in the liquid state. The isotropic coupling values obtained from such studies are given in Table 4, where they are compared with the calculated values of this study. Excellent agreement between theory and experiment is achieved in all cases except for the C1 hyperfine coupling. Our previous studies on the unsubstituted *p*-benzosemiquinone anion radical[7] have also indicated that this position shows the largest error when compared with the experimental value. For the unsubstituted semiquinone, the experimental value is sensitive to the concentration of the hyrogen-bonding solvent used. In the durosemiquinone experimental study of ref 19, no details are given of the concentration of solvent alcohol used or of how the sign of this coupling was determined. For the unsubstituted *p*-benzosemiquinone anion, the sign of this coupling constant is

negative for all alcohol solvents tested.[7] It acquires a small positive value only in 100% aqueous solutions. For a valid comparison between theory and experiment to be made for this hyperfine coupling, it will be necessary to study the experimental coupling in alcohol solvents of varying concentration. The methyl group ^{13}C hyperfine coupling has been reliably determined by ENDOR studies[20] and shows excellent agreement with the calculated value, Table 4. From Table 3 we can see that this coupling also has low anisotropy, being principally isotropic in nature. Low anisotropy is particularly favorable for ENDOR detection and explains why this couplings has been observed in ^{13}C natural abundance using ENDOR.[20]

Of perhaps greater interest are the hyperfine couplings obtained in frozen solutions and those obtained for reaction center preparations where DQ occupies the Q_a binding site.[3,9,10] In these immobilized states, the anisotropic components contribute to the resonances observed and one obtains the total tensor components, i.e., isotropic plus anisotropic. EPR studies have been successful in obtaining the largest tensor component for ^{17}O-enriched DQ both in frozen alcohol solution and in the Q_a binding site of *Rb. sphaeroides*.[10] In the alcohol matrix only one hyperfine coupling was observed. This resonance was attributed to the equivalent carbonyl oxygen atoms of the semiquinone. An absolute value of 82 MHz was reported.[10] Adding the isotropic and anisotropic values of DQ−4CH_3OH, Tables 2 and 3, we obtain the corresponding calculated value of −83 MHz for both O1 and O4. The agreement between theory and experimental data is clearly excellent in this case. For DQ substituted into the Q_a binding site, an inequivalence of the two oxygen atoms was noted and two different hyperfine couplings were reported having values of 80 and 93 MHz. This inequivalence of the oxygen atoms is well reproduced by the DQ−IM complex. Adding the ^{17}O isotropic and anisotropic values of DQ−IM, Tables 2 and 3, two values of −96 MHz (O1) and −84 MHz (O4) are obtained. This agreement suggests that the inequivalence of the DQ oxygen atoms in the Q_a binding site is caused by asymmetric hydrogen bonding to the O4 oxygen atom. The most likely candidate for such hydrogen bonding is the HIS M219 residue, which has been shown to be within hydrogen-bonding distance of the O4 oxygen atom of the Q_a quinone in *Rb. sphaeroides*.[21]

^1H principal hyperfine tensor values have also been obtained for DQ in frozen alcohol solutions and also upon substitution into the Q_a binding site of *Rb. sphaeroides*. In the frozen alcohol matrix an axial tensor is obtained for the 12 equivalent protons with principal values of 7.7 and 4.5 MHz.[9] Even in the frozen alcohol matrix, free rotation of the methyl groups is possible, resulting in an average tensor for each methyl group. For calculation purposes we have used a fixed orientation of the methyl group protons and averaged the three values obtained for each group. For DQ−4CH_3OH this procedure gives us total principal hyperfine tensor values values of +7.7, +4.1, and +3.2 for the methyl groups. The agreement with the experimental determination is quite satisfying considering the approximations used. On substituting DQ into the Q_a binding site, the equivalence of the four methyl group couplings is removed, and three sets of axial tensors have been reported: {6.0, 3.3 MHz}, {8.5, 5.2 MHz}, and {9.3, 6.0 MHz}.[3,10] We have obtained the methyl group tensors for the DQ−IM complex similarly to the DQ−4CH_3OH discussed above. Similar to that observed experimentally for the Q_a binding site durosemiquinone the equivalence of the methyl group tensors is removed and four methyl group tensors are calculated as follows: CH_3(2) {11.3, 7.6, 6.6}; CH_3(3) {5.3, 2.0, 1.1}; CH_3(5) {5.0, 1.4, 0.9}; CH_3-(6) {10.1, 6.5, 5.5}.

The methyl groups at positions 2 and 6 are located at positions of high π density, which leads to the increased values compared with DQ−4CH_3OH. The 3 and 5 couplings are from methyl groups attached to low spin density positions. The good agreement with the reaction center experimental trend is again indicative of asymmetric hydrogen bonding to the semiquinone in the semiquinone in the Q_a site of *Rb. sphaeroides*. The calculated total principal hyperfine coupling values for the hydrogen-bonding protons of DQ-4CH_3OH are {7.0, −4.8, −5.2}, {7.1, −5.0, −5.3}, {6.4, −3.9, −4.0}, and {6.9, −4.6, −4.9}. These differ considerably from the in-plane hydrogen-bonding tensors for the unsubstituted *p*-benzosemiquinone anion radical,[7,13] which lead to essentially pure anisotropic coupling. Out-of-plane hydrogen bonding leads to a significant *negative* isotropic coupling component in contrast with the positive value recently derived.[22] The experimental ^1H ENDOR data in ref 22 clearly needs to be reassessed on the basis of this information. The experimentally observed band having a hyperfine coupling of 0.98 MHz and assigned to these hydrogen bonds in ref 22 is unlikely to arise from the direct hydrogen bond to the semiquinone carbonyl oxygen. The broad band observed extending over a hyperfine coupling range of 4.0−7.0 MHz is in good agreement with the values calculated here.

Recently EPR studies have revealed the ^{13}C total principal hyperfine tensor values for the C1 and C4 carbon atom positions for the related ubisemiquinone anion radical both in a frozen alcohol matrix and in the Q_a binding site.[4] Whereas essentially equivalent values were obtained for the C1 and C4 positions in the frozen alcohol matrix, the values were different in the reaction center binding site with an increased C4 value and a decreased C1 value compared with the frozen alcohol matrix. This trend is again similar to that found for the DQ−IM radical complex where hydrogen bonding to the O4 atom by the imidazole leads to an increase in spin density at C4 at the expense of the C1 position. This is reflected in increased values of the anisotropic principal values for C4 and decreased values for C1, Table 2.

Conclusions

These studies have once again demonstrated the power of hybrid density functional methods in the calculation of isotropic and anisotropic hyperfine couplings for free radical species. Examination of the spin density distribution in symmetrically hydrogen-bonded and asymmetrically hydrogen-bonded durosemiquinone anion radical and comparison with experimental EPR and ENDOR data lead us to conclude that the semiquinone formed at the Q_a site of *Rb. sphaeroides* is asymmetrically hydrogen bonded, which leads to an alteration in its spin density distribution compared with the symmetrically hydrogen-bonded state. From the reaction center crystal structure of *Rb. sphaeroides*, the most likely candidate for a hydrogen bond to the O4 oxygen atom is HIS M219.[21] The crystal structure also indicates that a hydrogen bond is also formed to the O1 atom via a peptide NH link. It is unclear at present whether this link is broken on semiquinone radical formation due to a closer interaction of the semiquinone with HIS M219; i.e., the semiquinone moves toward the histidine residue. We plan to investigate such effects as well as the influence of the positively charged Fe^{2+}, which is an additional ligand to the HIS M219.

References and Notes

(1) *Functions of Quinones in Energy Conserving Systems*; Trumpower, B. I., Ed.; Academic Press: New York, 1986.

(2) Okamura, M. Y.; Feher, G. *Annu. Rev. Biochem.* **1992**, *61*, 861.
(3) Feher, G.; Isaacson, R. A.; Okamura, M. Y.; Lubitz, W. In *Antennas and Reaction Centers of Photosynthetic Bacteria*; Michel-Beyerle, M. E. Ed.; Springer-Verlag: Berlin, 1985; pp 174−189.
(4) van den Brink, J. S.; Spoyalov, A. P.; Gast, P.; van Liemt, W. B. S.; Raap, J.; Lugtenburg, J.; Hoff, A. J. *FEBS Lett.* **1994**, *353*, 273.
(5) Breton, J.; Burie, J.-R.; Boullais, C.; Berger, G.; Nabedryck, E.; Mioskowski, C. *Biochemistry* **1994**, *33*, 14378.
(6) van Liemt, W. B. S.; Boender, G. J.; Gast, P.; Hoff, A. I.; Lugtenberg, I.; de Groot, H. M. J. *Biochemistry* **1995**, *34*, 10229.
(7) O'Malley, P. J. *J. Phys. Chem. A* **1997**, *101*, 6334.
(8) O'Malley, P. J. *J. Phys. Chem. A*, in press.
(9) O'Malley, P. J.; Babcock, G. T. *J. Chem. Phys.* **1984**, *80*, 3912.
(10) Lubitz, W.; Abresch, E. C.; Debus, R. J.; Isaacson, R. A.; Okamura, M. Y.; Feher, G. *Biochim. Biophys. Acta* **1985**, *808*, 464.
(11) Adamo, C.; Barone, V.; Fortunelli, V. *J. Chem. Phys.* **1995**, *102*, 1689.
(12) O'Malley, P. J.; Ellson, D. A. *Chem. Phys. Lett.* **1996**, *269*, 492.
(13) O'Malley, P. J. *Chem. Phys. Lett.* **1996**, *262*, 797.
(14) Barone, V. In *Recent Advances in Density Functional Methods*; Chong, D. P., Ed., World Scientific Publishing: Singapore, 1995.
(15) Becke, A. D. *J. Chem. Phys.* **1993**, *98*, 5648.
(16) Frisch, M. J.; Trucks, G. W.; Schlegel, H. B.; Gill, P. W.; Johnson, B. G.; Wong, M. W.; Foresman, J. B.; Robb, M. A.; Head-Gordon, M.; Replogle, E. S.; Gomperts, R.; Andres, J. L.; Raghvachari, K.; Binkley, J. S.; Gonzalez, C.; Martin, R. L.; Fox, D. J.; Defrees, D. J.; Baker, J.; Stewart, J. J. P.; Pople, J. A. *GAUSSIAN 94*; Gaussian Inc.: Pittsburgh, PA, 1995.
(17) SPARTAN 4.1.1, Wavefunction Inc., California, 1995.
(18) Gordy, W. *Theory and Applications of Electron Spin Resonance*; Wiley: New York, 1980.
(19) Das, M. R.; Connor, H. D.; Leniart, D. S.; Freed, J. H. *J. Am. Chem. Soc.* **1970**, *92*, 2258.
(20) Kirste, B. *Magn. Reson. Chem.* **1987**, *25*, 166.
(21) Erlmer, U.; Fritzsch, G.; Buchanan, S.; Michel, H. *Structure* **1994**, *2*, 925.
(22) MacMillan, F.; Lendzian, F.; Lubitz, W. *Magn. Reson. Chem.* **1995**, *33*, 581.